Effect of Npt2b deletion on intestinal and renal inorganic phosphate (Pi) handling

Kayo Ikuta[1], Hiroko Segawa[1], Shohei Sasaki[1], Ai Hanazaki[1], Toru Fujii[1], Aoi Kushi[1], Yuka Kawabata[1], Ruri Kirino[1], Sumire Sasaki[1], Miwa Noguchi[1], Ichiro Kaneko[1], Sawako Tatsumi[1], Otoya Ueda[2], Naoko A.Wada[2], Hiromi Tateishi[3], Mami Kakefuda[3], Yosuke Kawase[3], Shuichi Ohtomo[2], Yasuhiro Ichida[2], Akira Maeda[2], Kou-ichi Jishage[2, 3], Naoshi Horiba[2], Ken-ichi Miyamoto[1]

[1]Department of Molecular Nutrition, Institute of Biomedical Sciences, Tokushima University Graduate School, Tokushima, Tokushima, Japan

[2]Chugai Pharmaceutical Co., Ltd., Research Division, Fuji Gotemba Research Labs., 1-135, Komakado, Gotemba, Shizuoka, Japan.

[3]Chugai Research Institute for Medical Science, Inc. 1-135, Komakado, Gotemba, Shizuoka, Japan.

Running Head:
Conditional deletion of Npt2b in phosphate transport

Address for correspondence:
Hiroko Segawa PhD
Department of Molecular Nutrition, Institute of Biomedical Sciences
Tokushima University Graduate School
3-18-15 Kuramoto-Cho, Tokushima City 770-8503, Japan
Phone: 81-88-633-7082; Fax: 81-88-633-7082
E-mail: segawa@tokushima-u.ac.jp

Word count; 3787

Abstract

Background Hyperphosphatemia is common in chronic kidney disease and is associated with morbidity and mortality. The intestinal Na^+-dependent phosphate transporter Npt2b is thought to be an important molecular target for the prevention of hyperphosphatemia. The role of Npt2b in the net absorption of inorganic phosphate (Pi), however, is controversial.

Methods In the present study, we made tamoxifen-inducible Npt2b conditional knockout (CKO) mice to analyze systemic Pi metabolism, including intestinal Pi absorption.

Results Although the Na^+-dependent Pi transport in brush-border membrane vesicle uptake levels were significantly decreased in the distal intestine of Npt2b CKO mice compared with control mice, plasma Pi and fecal Pi excretion levels were not significantly different. Data obtained using the intestinal loop technique showed that Pi uptake in Npt2b CKO mice was not affected at a Pi concentration of 4 mM, which is considered the typical luminal Pi concentration after meals in mice. Claudin, which may be involved in paracellular pathways, as well as claudin-2, 12, and 15 protein levels were significantly decreased in the Npt2b CKO mice. Thus, Npt2b deficiency did not affect Pi absorption within the range of Pi concentrations that normally occurs after meals.

Conclusion These findings indicate that abnormal Pi metabolism may also be involved in tight junction molecules such as Cldns that are affected by Npt2b deficiency.

Keywords:
Intestine, Trans-cellular transport Para-cellular transport,

Introduction

Hyperphosphatemia is a serious consequence of late-stage chronic kidney disease that leads to increased cardiovascular morbidity and mortality, particularly in patients on dialysis[1-3]. Recent epidemiologic studies demonstrated that increased serum inorganic phosphate (Pi) concentrations, even those within the normal range, can be an independent risk factor for cardiovascular morbidity and mortality in the general population as well as in patients with chronic kidney disease[1-3]. Current strategies for treating hyperphosphatemia in dialysis patients include dietary Pi restriction and oral Pi binders, although these treatments, if used aggressively, can lead to malnutrition, adverse gastrointestinal effects, and poor compliance with all medications, particularly in the elderly. Furthermore, patient adherence to taking Pi binders is poor, due in part to the pill burden (12 or more tablets per day are often required in a background of polypharmacy), timing of ingestion around mealtimes, and gastrointestinal side effects such as constipation and abdominal bloating[1-3]. Therefore, the development of a small molecular compound, such as a Pi transport inhibitor, is desired.

The cellular transport pathway in the small intestine requires Na^+-dependent Pi transporters, including NaPi-IIb (SLC34A2, Npt2b)[4]. In a renal failure model of adenine administration in intestinal Npt2b knockout (KO) mice, serum Pi concentrations are significantly reduced[5-7]. Based on such studies using Npt2b KO mice, intestinal Npt2b is an important target for the treatment of CKD-associated hyperphosphatemia[5-7]. The role of Npt2b in net Pi absorption and the effect of Npt2b inhibitors for the treatment of hyperphosphatemia, however, remain controversial.

More recent studies revealed that tenapanor is not a Pi binder, but rather a small molecule inhibitor of the sodium/hydrogen exchanger NHE3, which plays an important role in sodium and fluid homeostasis but has no direct effect on the sodium dependent Pi co-transporter Npt2b and does not directly bind intestinal Pi ions[8]. In addition, previous studies reported that NHE3 inhibitors affect tight junction modifications and barrier

function[9]. As described above, abnormal Pi metabolism in Npt2b KO mice, in addition to suppression of Na^+-dependent Pi transport, may affect the expression of other factors involved in intestinal ion transport.

In the present study, we made tamoxifen-inducible Npt2b conditional KO (CKO) mice, and analyzed their systemic Pi metabolism, including intestinal Pi absorption. We further investigated the expression of tight junction proteins in the small intestine in Npt2b CKO mice. Our findings indicate that various factors may be involved in the intestinal Pi handling abnormalities of Npt2b CKO mice.

Materials and Methods

Animals and Diet

Mice were generated and maintained under pathogen-free conditions, and handled in accordance with the Guidelines for Animal Experimentation of Tokushima University School of Medicine and with the Guidelines for the Care and Use of Laboratory Animals at Chugai Pharmaceuticals. Mice were weaned at 3 weeks of age, and provided free access to water and standard mouse chow (1.12% Ca and 0.9% Pi; Oriental, Osaka, Japan).

Generation of the Npt2b CKO mouse line

The targeting vector, which was constructed by BAC engineering[10-12], was electroporated into mouse embryonic stem (ES) cells (Figure 1A, supplementary methods and supplementary Figure 1). *Npt2b* CKO mice were generated from correctly targeted ES cell clones, and intercrossed with CAG-*MerCreMer* transgenic mice[13] to establish a tamoxifen-inducible *Npt2b* CKO mouse line. Genotyping was performed by genomic polymerase chain reaction (PCR) in the breeding process. Primer sets to detect the CKO alleles and the *MerCreMer* transgene are listed in Table 1.

Induction of gene disruption in the Npt2b CKO mice

In the present study, the Cre recombinase was activated upon administration of tamoxifen citrate salt (Sigma-Aldrich, St. Louis, MO). Tamoxifen (3% wt:wt) was administered to mice in standard mouse chow for 7 days, and the mice were allowed to recover for 7 days before the study.

Metabolic cages to collect urine and fecal samples

Mice were individually caged to collect 24-h urine and fecal samples. Fecal samples were ashed according to a modified protocol[14]. The fecal samples were collected and placed into beakers to dry at 110°C for no more than 24 h. The samples were then ashed at 250°C for 3 h and at 550°C for 24 h in a muffle furnace. The samples were cooled, weighed, and digested in HCl with heat, and the sample volume was standardized to 5 ml.

Concentrations of Pi, Ca, Cr, and $1,25(OH)_2D_3$

Concentrations of inorganic Pi, calcium (Ca), and creatinine (Cr) were determined using commercial kits (Wako, Osaka, Japan)[5,15]. Plasma $1,25(OH)_2D_3$ concentrations were determined using the $1,25\text{-}(OH)_2$ Vitamin D ELISA Kit (Immundiagnostik, Bensheim, Germany)[16].

Pi levels in the intestinal lumen

Mice were anesthetized 3 h after the lights were turned off or on in the 12 h light/12 h dark cycle. 1) The gastrointestinal contents were washed out from each region of the gastrointestinal tract (proximal, middle, and distal intestine) with distilled water and vortexed vigorously[17]. Solid contents from the distal intestine and colon were diluted and homogenized for 10 s. Then, samples were centrifuged at 3000 x g for 10 min and an aliquot of the supernatant was used to determine the free Pi concentration using a commercial kit (Wako). 2) The mouse abdomen was opened to obtain a sample of residual solid contents and water from the proximal, middle, and distal intestinal segments[18,19]. Solid contents, including feces and food, were obtained with

forceps. Because the water volume remaining in each segment was very small, luminal water was sampled using a cotton ball by carefully wiping the surface of the intestinal membrane in each region. Then, the cotton ball was placed in the tube and centrifuged at 13,000 x g for 5 min and an aliquot was used to determine free Pi concentration using a commercial kit (Wako).

RNA extraction and cDNA synthesis

Total RNA was extracted from the intestine of mice using ISOGEN (Wako, Osaka Japan) according to the manufacturer's instructions. After treatment with DNase (Invitrogen, Carlsbad, CA), cDNA was synthesized using the Moloney murine leukemia virus, reverse transcriptase (Invitrogen), and oligo(dT)12-18 primer.

Quantitative PCR

Quantitative PCR was performed using StepOnePlus™ (Applied Biosystems, Foster City, CA). The reaction mixture comprised 10 μl of SYBR Premix Ex Taq, ROX Reference Dye II (Perfect Real Time, Takara, Osaka, Japan) with specific primers. The PCR reactions were initiated by denaturation at 95°C for 30s, annealing at 95°C for 5s, and 60°C for 30 s. Data were evaluated with SDS v. 1.2X with RQ software. PCR primer sequences are shown in Table 2.

Preparation of brush-border membrane vesicles

Brush-border membrane vesicles (BBMVs) were prepared from the mouse intestinal mucosa and kidneys using modified Ca^{2+} precipitation methods[20]. Intestinal mucosa or macroscopic dissections of a kidney were homogenized in a ice-cold homogenate buffer (50 mM mannitol, 10 mM Tris/Hepes pH 7.5) with a blender for 120 s. $CaCl_2$ was added to the homogenized tissues to obtain a final concentration 100 mM $CaCl_2$, and the samples were mixed by inversion and the tubes placed on ice for 15 min. The tubes were centrifuged at 5000

rpm at 4℃ for 15 min using HIMAC SCR20B (Hitachi Koki Co., Ltd, Tokyo, Japan). The supernatant was decanted into the new centrifugation tube and centrifuged at 18,000 rpm at 4°C for 30 min using HIMAC SCR20B (Hitachi Koki Co., Ltd). The pellet was suspended in a 1 ml of suspension buffer (300 mM mannitol, 10 mM Tris/HEPES pH 7.5), centrifuged again, and resuspended in a small amount of suspension buffer.

Preparation of crude membrane

Crude membranes were prepared according to a previously described method. [21] Intestine homogenates in 0.3 M sucrose containing protease inhibitor cocktail tablets (Complete Mini, EDTA-free; Roche) were centrifuged at 600 g for 10 min, and the supernatant was then centrifuged at 105,000 g for 45 min, and the membrane pellet was used for claudins Western blotting analysis.

Immunoblotting analysis

Protein samples were placed in sample buffer in the presence of 2-mercaptoethanol and subjected to 8% (NaPi transporters) or 12% (Claudins) sodium dodecyl sulfate-polyacrylamide gel electrophoresis. The separated proteins were transferred by electrophoresis to Immobilon-P polyvinylidene difluoride membranes (Millipore, Billerica, MA) and then treated with diluted affinity-purified anti-Npt2b antibody (Alpha Diagnostic International, San Antonio, TX)[5], and anti-Npt2a and Npt2c antibodies were described as previously[5,15]. Claudin 2 (Abcam, Cambridge, MA), 4 (Thermo Fisher Scientific Inc., Waltham, MA), 12 (Invitrogen), and 15 (Thermo Fisher Scientific Inc.) antibodies were purchased respectively.

Mouse anti-actin monoclonal antibody (Chemicon, Temecula, CA) was used as an internal control. Horseradish peroxidase-conjugated anti-rabbit or anti-mouse IgG was utilized as the secondary antibody (Jackson Immuno

Research Laboratories, Inc, West Grove, PA), and signals were detected using Immobilon Western Chemiluminescent HRP Substrate (Millipore).

BBMV transport study and everted sac technique

BBMV Pi transport activity was measured in the mouse small intestine and kidney using a rapid filtration technique, as described previously[20]. A modified everted sac technique was used to evaluate the Pi transport activity in the small intestine of the mice[20]. The intestine was divided into two segments, proximal and distal, everted using a spatula, and fastened with string. The sac was filled with solution (128 mM NaCl or choline Cl, 4.7 M KCl, 2.5 mM $CaCl_2$, and 1.2 mM KH_2PO_4, pH 7.4). The sacs were then incubated in a flask with the uptake solution (128 mM NaCl or choline Cl, 4.7 M KCl, 2.5 mM $CaCl_2$, and 1.2 mM or 4 mM KH_2PO_4, pH. 7.4) containing ^{32}P (0.25 mCi/ml) for 30 min under an atmosphere of 95% O_2/5% CO_2 at 37°C. After incubation, the sac was removed from the flask and washed in cold saline. The sac was cut open and the uptake solution drained into a vial for counting in a liquid scintillation counter.

Statistical Analysis

Data are expressed as means ± SE. Differences among multiple groups were analyzed by ANOVA followed by Scheffe test. The significance of differences between two experimental groups was established by ANOVA followed by Student's *t* test. A *P* value of less than 0.05 was considered significant.

Results

Generation of Npt2b CKO mice

A tamoxifen-inducible*Npt2b* CKO (*Npt2b*$^{lox/lox}$, CAG-*MerCreMer*) mouse line was established as depicted in Figure 1A and Supplementary Figure 1. A representative result of genotyping is shown in Figure 1B. The

Npt2b conditional allele was detected as a signal at 1.8 kb, while the wild-type allele was detected at 236 bp. The CAG-MerCreMer transgenic allele was detected as a signal at 0.9 kb. After tamoxifen administration, deletion of Npt2b mRNA and reduction of Npt2b protein in the proximal and distal intestine of Npt2b CKO mice was confirmed by reverse transcription (RT) -PCR and Western blotting (Figure 1C and 1D). The RT-PCR of wild-type Npt2b products were detected as a 398-bp band in the proximal and distal intestine of both the Npt2b CKO mice and wild type mice without tamoxifen administration. In contrast, RT-PCR products derived from Npt2b disrupted allele were detected as a 140-bp band in the Npt2b CKO mice after tamoxifen administration. Npt2b protein level was much lower in tamoxifen-administered Npt2b CKO mice than that before tamoxifen administration (Figure 1D). Npt2b mRNA was detected in several tissues such as the lung, kidney, and liver, as described previously[22]. Although the mRNA transcribed from the Npt2b disrupted allele was also detected in the lung, kidney, and liver (data not shown), Npt2b disrupted allele does not contain the coding region of exons 5 and 6, which cannot produce mature Npt2b protein due to the frame shift. Furthermore, no calcification was detected in the lung in our Npt2b CKO mice (data not shown).

Physiologic data of Npt2b CKO mice

The ionized Ca levels were significantly increased in Npt2b CKO mice after knockout induction compared with those before induction (referred as the controls) (Figure 2A). In contrast, there was no difference in the plasma Pi concentration between the control and Npt2b CKO mice (Figure 2B). Furthermore, the urine volume and urinary Ca excretion levels were significantly higher and the urinary Pi excretion level was significantly lower in the Npt2b CKO mice than in control mice (Figure 2C-2E). Fecal Pi and Ca excretion levels, however, were not different in Npt2b CKO mice compared with those in control mice (Figure 2F and 2G). Plasma $1,25(OH)_2D_3$ concentrations were significantly higher in Npt2b CKO mice than those in control mice (Figure 2H).

Intestinal and renal brush-border membrane Pi transport activity in Npt2b CKO mice

Intestinal Pi transport activity was examined using BBMVs (Figure 3). Na^+-independent Pi transport activity was not altered in Npt2b CKO mice compared with control mice (Figure 3A). In contrast, Na^+-dependent Pi transport activity levels were significantly lower in Npt2b CKO mice than in control mice (Figure 3B). In the kidney, Pi transport activity was slightly, but not significantly, lower in Npt2b CKO mice than in control mice (Figure 3C). Furthermore, there were no significant differences in the renal Npt2a and Npt2c protein expression concentrations between control and Npt2b CKO mice (Figure 3D).

Intestinal luminal Pi concentration in wild-type mice

Marks et al. reported that the Pi concentration in the gastrointestinal region of rats is in the millimolar range[17]. In the present study, we measured the Pi concentration in the proximal, middle, and distal regions of mice using two methods (Figure 4). First, we measured the Pi concentration at 11:00 in the morning and at 11:00 at night following Marks's protocol[17]. The intestinal luminal Pi concentration was significantly higher in the proximal intestine than in the distal intestine at both time-points (Figure 4A). At both time-points, the Pi concentration was 1.5-2 mM in the proximal intestine, approximately 1 mM in the middle intestine, and 0.3-0.5 mM in the distal intestine (Figure 4A). We then measured the intestinal luminal Pi concentration at 11:00 in the morning and at 11:00 at night following another protocol. In this method, a modification of Masaoka's[18] and Tanaka's[19] protocol, the luminal water was carefully collected using a cotton ball to wipe the surface of the intestinal membrane. Luminal Pi concentrations in the middle and distal intestine were significantly higher in the morning than at night (Figure 4B). Furthermore, the concentration of Pi in each region was much higher (15-40 mM) than those shown in Figure 4A, which were measured following Marks's protocol. Thus, the intestinal luminal surface Pi concentration was high (Figure 4B).

Intestinal Pi transport activity determined using the everted sac technique in Npt2b CKO mice

Next, ^{32}P transport from the mucosal to the serosal side was examined using the everted sac technique in Npt2b CKO mice (Figure 5). The study was conducted under two conditions. The first study examined ^{32}P transport in solution containing 1 mM Pi. Although Na^+-independent Pi transport activity in the proximal intestine of Npt2b CKO mice was slightly, but significantly, higher than that in control mice, it was slightly but significantly lower in the distal intestine of Npt2b CKO mice compared with control mice (Figure 5A and 5B). Na^+-dependent Pi transport activity in the proximal intestine was not significantly different between control and Npt2b CKO mice (Figure 5A). In contrast, Na^+-dependent Pi transport activity in the distal intestine was significantly lower in Npt2b CKO mice than in control mice (Figure 5B). The second study examined ^{32}P transport in solution containing 4 mM Pi. Under these conditions, the Na^+-independent or -dependent Pi transport activities were not significantly different between control and Npt2b CKO mice (Figure 5C and 5D).

Intestinal transporter and claudin mRNA expression in Npt2b CKO mice

Intestinal Pi is thought to be absorbed via two pathways, a transcellular pathway involving a transporter, such as Npt2b or PiT1, and a paracellular pathway[23,24]. The paracellular Pi transport mechanism, however, is poorly characterized. In the present study, due to the lack of intestinal Npt2b protein expression, the BBMV and everted sac intestinal Na^+-dependent transport activity assays showed that the Pi concentration was significantly decreased in Npt2b CKO mice compared with control mice, and there were no significant decreases in the plasma Pi and fecal Pi excretion levels in Npt2b CKO mice compared with control mice. Based on these results, to clarify the mechanism that compensates for the decreased Pi absorption due to the loss of Npt2b, the mRNA expression levels of related molecules in the transcellular system excluding Npt2b or the paracellular pathway system were examined in the Npt2b CKO mouse intestine. The proximal and distal intestine NHE3,

PiT1, and PiT2 mRNA expression levels did not differ significantly between control and knockdown mice (Figure 6A-C). Furthermore, claudin-3, -8, -12, -15, and -25 mRNA expression levels were significantly decreased in Npt2b CKO mice after induction compared with those in control mice (Figure 6D-K). In addition, the amount of each caludin protein was measured using the available antibodies. In the Npt2b CKO mice, the levels of claudin -2, -12, and -15 protein were significantly reduced (Figure 7).

Discussion

In the present study, we investigated Pi metabolism in tamoxifen-induced Npt2b CKO mice. Sabbagh et al. reported that intestinal Npt2b deletion affects renal Pi transport[7]. In the present study, Npt2b KO mice had hypophosphaturia, but no adaptation of the renal Npt2a and Npt2c protein was observed. In addition, lung calcification was not prominent in our Npt2aKO mice. The increase in the plasma $1,25(OH)_2D_3$, however, indicates that deletion of Npt2b reduces intestinal Pi absorption in Npt2b CKO mice. Consistent with Sabbagh et al.'s data, conditional deletion of Npt2b enhanced renal Pi reabsorption and caused hypophosphaturia[7]. The urine volume and urinary Ca excretion levels were significantly higher in Npt2b CKO mice. These phenotypes are observed in mice with low Pi status as reported previously[25,26]. In addition, Npt2b-mediated transport in the mouse ileum accounts for ~90% of its total Na^+-dependent Pi absorption across the BBM[7]. They analyzed Npt2b CKO mice and determined that the transporter accounts for only ~50% of the total intestinal transepithelial Pi absorption in response to a dietary Pi load[7]. In the present study, we also analyzed intestinal Pi transport based on BBMV uptake and an everted sac assay. The everted sac assay is used to evaluate intestinal Pi absorption via the transcellular and paracellular pathways. In a previous report, intestinal Pi absorption (low concentration, at 1.2 mM Pi) significantly decreases Na^+-dependent Pi transport in the everted sac method[7]. In that report, they suggested that Npt2b accounts for 50% of the Na^+-dependent Pi transport in the small intestine. Information on the luminal free Pi concentration

available for absorption following ingestion of a normal diet indicates a greater increase than 1.2 mM Pi. Recently, Marks suggested that the Pi concentration in the small intestinal lumen is approximately 5-11 mM in rats[17]. Although there are considerable variations depending on the time of day, we also confirmed that the luminal Pi concentration in mice with a normal diet was at least 4 mM. In addition, functional analysis of Npt2b in Xenopus oocytes shows an apparent Km for Pi of ~15 μM[27], suggesting that the luminal Pi concentration after food intake is saturable for intestinal Npt2b transport function. Previous studies concluded that paracellular transport is the dominant absorption pathway for high luminal Pi concentrations in both rodents and humans[6,28,29]. The everted sac assay showed a significant reduction in Na^+-independent Pi transport activity in the ileum in Npt2b CKO mice. These findings suggest that Pi transport by the paracellular pathway was also decreased in Npt2b CKO mice.

A recent study demonstrated that an NHE3 inhibitor (tenapanor) markedly reduces intestinal Pi absorption[8]. In 5⁄6 nephrectomy rats, tenapanor also markedly reduces urinary Pi excretion as well as serum Pi, calcium, creatinine, and FGF23 concentrations[8]. The mechanism is unclear, and the details of Pi absorption in rats administered tenapanor are unknown[8]. It may simply be the result of less passive Pi transport secondary to reduced water flux. One possibility is that the NHE3 inhibitor affects the tight junction proteins and inhibits the paracellular Pi transport pathway. Indeed, NHE3 KO mice have decreased intestinal calcium absorption[9]. In addition, in NHE3 KO mice, jejunal claudin-2 and -15 expression is significantly decreased[9]. NHE3 may reduce intestinal Pi absorption by inhibiting the paracellular pathway.

Tight junctions are the most apical component of the junctional complex between epithelial cells[30-33]. Tight junctions separate the cell membrane into the apical and basolateral domains for their critical role in regulating paracellular barrier permeability. Many claudins also have distinct charge-selectivity. Some claudins act as paracellular channels[30-33]. For example, claudin-2 and -15 are cation-selective, and claudin-17 is anion-selective[32]. Furthermore, claudin-8 is involved in regulating paracellular Na^+ permeability[34].

Claudin-2 and -12 are involved in Ca^{2+} permeability[35]. Double-knockout of claudin-2 and -15 reduces the paracellular flow of Na^{+} from the intestinal submucosa into the lumen and decreases the absorption of several Na^{+}-dependent nutrients, such as glucose, amino acids, etc[36]. Thus, the paracellular roles of claudins are related to the passive flow of several types of ions. In the present study, claudin-3, 8, 12, 15, and 25 mRNA levels were significantly decreased in the Npt2b CKO mice. In addition, the amount of each claudin protein was measured using the available antibodies. In the Npt2b CKO mice, the levels of claudin -2, -12, and -15 protein were significantly reduced. Changes in the expression of several claudins, however, might be related to intestinal paracellular Pi absorption. Alternatively, because Npt2b is expressed in various tissues, including the kidney, deletion of Npt2b in these organs may contribute to abnormal Pi metabolism. Further studies are needed to clarify the relationship between Pi absorption and claudins.

Finally, in the present study, we produced Npt2b CKO mice to analyze systemic Pi metabolism, including intestinal Pi absorption. Although Npt2b is an important molecule for intestinal Pi absorption at a low concentration of Pi, we suggest that other molecules are involved in the abnormal Pi metabolism observed in Npt2b CKO mice.

Acknowledgments

This work was supported by grants from the Ministry of Education, Culture, Sports, Science and Technology of Japan (26461254 to H.S. and 26293204 to K.M.), and The Salt Science Research Foundation (Japan). We thank Ms. Y. Oikawa, Ms. C. Honda, Mr. T. Tachibe, Ms. C. Goto, Mr. K. Matsumoto, Mr. K. Sato, Mr. M. Morita and Ms. S. Uchida for skillful cooperation in establishment of NaPi2b CKO mouse line. Furthermore, we are grateful to Drs. Sachiko Tsukita and Tamura Atsushi (Osaka University) for scientific discussion.

Conflict of interest

KI, HS, Shohei S, AH, TF, AK, YK, RK, Sumire S, MN, IK, ST, and KM have declared that no conflict of interest exists. OU, NW, SO, YI, AM, KJ and NH are employees of Chugai Pharmaceutical Co., Ltd.. HT, MK, YK and KJ are Chugai Research Institute for Medical Science, Inc..

Human and Animal Right

Mice were handled in accordance with the Guidelines for Animal Experimentation of Tokushima University School of Medicine and with the Guidelines for the Care and Use of Laboratory Animals at Chugai Pharmaceuticals. This article does not contain any studies with human participants.

References

1 Block GA, Kilpatrick RD, Lowe KA, Wang W, Danese MD: Ckd-mineral and bone disorder and risk of death and cardiovascular hospitalization in patients on hemodialysis. Clinical journal of the American Society of Nephrology : CJASN 2013;8:2132-2140.

2 Cannata-Andia JB, Martin KJ: The challenge of controlling phosphorus in chronic kidney disease. Nephrology, dialysis, transplantation : official publication of the European Dialysis and Transplant Association - European Renal Association 2016;31:541-547.

3 Vervloet MG, Sezer S, Massy ZA, Johansson L, Cozzolino M, Fouque D, Disease-Mineral E-EWGoCK, Bone D, the European Renal Nutrition Working G: The role of phosphate in kidney disease. Nature reviews Nephrology 2017;13:27-38.

4 Wagner CA, Hernando N, Forster IC, Biber J: The slc34 family of sodium-dependent phosphate transporters. Pflugers Archiv : European journal of physiology 2014;466:139-153.

5 Ohi A, Hanabusa E, Ueda O, Segawa H, Horiba N, Kaneko I, Kuwahara S, Mukai T, Sasaki S, Tominaga R, Furutani J, Aranami F, Ohtomo S, Oikawa Y, Kawase Y, Wada NA, Tachibe T, Kakefuda M, Tateishi H, Matsumoto K, Tatsumi S, Kido S, Fukushima N, Jishage K, Miyamoto K: Inorganic phosphate homeostasis in sodium-dependent phosphate cotransporter npt2b(+)/(-) mice. American journal of physiology Renal physiology 2011;301:F1105-1113.

6 Sabbagh Y, Giral H, Caldas Y, Levi M, Schiavi SC: Intestinal phosphate transport. Advances in chronic kidney disease 2011;18:85-90.

7 Sabbagh Y, O'Brien SP, Song W, Boulanger JH, Stockmann A, Arbeeny C, Schiavi SC: Intestinal npt2b plays a major role in phosphate absorption and homeostasis. Journal of the American Society of Nephrology : JASN 2009;20:2348-2358.

8 Labonte ED, Carreras CW, Leadbetter MR, Kozuka K, Kohler J, Koo-McCoy S, He L, Dy E, Black D, Zhong Z, Langsetmo I, Spencer AG, Bell N, Deshpande D, Navre M, Lewis JG, Jacobs JW, Charmot D: Gastrointestinal inhibition of sodium-hydrogen exchanger 3 reduces phosphorus absorption and protects against vascular calcification in ckd. Journal of the American Society of Nephrology : JASN 2015;26:1138-1149.

9 Pan W, Borovac J, Spicer Z, Hoenderop JG, Bindels RJ, Shull GE, Doschak MR, Cordat E, Alexander RT: The epithelial sodium/proton exchanger, nhe3, is necessary for renal and intestinal calcium (re)absorption. American journal of physiology Renal physiology 2012;302:F943-956.

10 Osoegawa K, Tateno M, Woon PY, Frengen E, Mammoser AG, Catanese JJ, Hayashizaki Y, de Jong PJ: Bacterial artificial chromosome libraries for mouse sequencing and functional analysis. Genome research 2000;10:116-128.

11 Zhang Y, Buchholz F, Muyrers JP, Stewart AF: A new logic for DNA engineering using recombination in escherichia coli. Nature genetics 1998;20:123-128.

12 Zhang Y, Muyrers JP, Testa G, Stewart AF: DNA cloning by homologous recombination in escherichia coli. Nature biotechnology 2000;18:1314-1317.

13 Tominaga T, Abe H, Ueda O, Goto C, Nakahara K, Murakami T, Matsubara T, Mima A, Nagai K, Araoka T, Kishi S, Fukushima N, Jishage K, Doi T: Activation of bone morphogenetic protein 4 signaling leads to glomerulosclerosis that mimics diabetic nephropathy. The Journal of biological chemistry 2011;286:20109-20116.

14 Silva IV, Cebotaru V, Wang H, Wang XT, Wang SS, Guo G, Devuyst O, Thakker RV, Guggino WB, Guggino SE: The clc-5 knockout mouse model of dent's disease has renal hypercalciuria and increased bone turnover. Journal of bone and mineral research : the official journal of the American Society for Bone and Mineral Research 2003;18:615-623.

15 Segawa H, Onitsuka A, Kuwahata M, Hanabusa E, Furutani J, Kaneko I, Tomoe Y, Aranami F, Matsumoto N, Ito M, Matsumoto M, Li M, Amizuka N, Miyamoto K: Type iic sodium-dependent phosphate transporter regulates calcium metabolism. Journal of the American Society of Nephrology : JASN 2009;20:104-113.

16 Yoon JY, Woo SI, Kim H, Sun YH, Hahn YS: Fractional exhaled nitric oxide and forced expiratory flow between 25% and 75% of vital capacity in children with controlled asthma. Korean journal of pediatrics 2012;55:330-336.

17 Marks J, Lee GJ, Nadaraja SP, Debnam ES, Unwin RJ: Experimental and regional variations in na+-dependent and na+-independent phosphate transport along the rat small intestine and colon. Physiological reports 2015;3

18 Masaoka Y, Tanaka Y, Kataoka M, Sakuma S, Yamashita S: Site of drug absorption after oral administration: Assessment of membrane permeability and luminal concentration of drugs in each segment of gastrointestinal tract. European journal of pharmaceutical sciences : official journal of the European Federation for Pharmaceutical Sciences 2006;29:240-250.

19 Tanaka Y, Goto T, Kataoka M, Sakuma S, Yamashita S: Impact of luminal fluid volume on the drug absorption after oral administration: Analysis based on in vivo drug concentration-time profile in the gastrointestinal tract. Journal of pharmaceutical sciences 2015;104:3120-3127.

20 Furutani J, Segawa H, Aranami F, Kuwahara S, Sugano M, Bannai K, Yamato H, Ito M, Miyamoto K: Dietary inorganic phosphorus regulates the intestinal peptide transporter pept1. Journal of renal nutrition : the official journal of the Council on Renal Nutrition of the National Kidney Foundation 2013;23:e11-20.

21 Thorens B, Sarkar HK, Kaback HR, Lodish HF: Cloning and functional expression in bacteria of a novel glucose transporter present in liver, intestine, kidney, and beta-pancreatic islet cells. Cell 1988;55:281-290.

22 Hilfiker H, Hattenhauer O, Traebert M, Forster I, Murer H, Biber J: Characterization of a murine type ii sodium-phosphate cotransporter expressed in mammalian small intestine. Proceedings of the National Academy of Sciences of the United States of America 1998;95:14564-14569.

23 Marks J, Debnam ES, Unwin RJ: The role of the gastrointestinal tract in phosphate homeostasis in health and chronic kidney disease. Current opinion in nephrology and hypertension 2013;22:481-487.

24 Segawa H, Shiozaki Y, Kaneko I, Miyamoto K: The role of sodium-dependent phosphate transporter in phosphate homeostasis. Journal of nutritional science and vitaminology 2015;61 Suppl:S119-121.

25 Andrade L, Reboucas NA, Seguro AC: Down-regulation of na+ transporters and aqp2 is responsible for acyclovir-induced polyuria and hypophosphatemia. Kidney international 2004;65:175-183.

26 Procino G, Carmosino M, Tamma G, Gouraud S, Laera A, Riccardi D, Svelto M, Valenti G: Extracellular calcium antagonizes forskolin-induced aquaporin 2 trafficking in collecting duct cells. Kidney international 2004;66:2245-2255.

27 Forster IC, Virkki L, Bossi E, Murer H, Biber J: Electrogenic kinetics of a mammalian intestinal type iib na(+)/p(i) cotransporter. The Journal of membrane biology 2006;212:177-190.

28 Mc HG, Parsons DS: The absorption of inorganic phosphate from the small intestine of the rat. Quarterly journal of experimental physiology and cognate medical sciences 1956;41:398-412.

29 Breves G, Schroder B: Comparative aspects of gastrointestinal phosphorus metabolism. Nutrition research reviews 1991;4:125-140.

30 Barmeyer C, Schulzke JD, Fromm M: Claudin-related intestinal diseases. Seminars in cell & developmental biology 2015;42:30-38.

31 Krug SM, Schulzke JD, Fromm M: Tight junction, selective permeability, and related diseases. Seminars in cell & developmental biology 2014;36:166-176.

32 Lu Z, Ding L, Lu Q, Chen YH: Claudins in intestines: Distribution and functional significance in health and diseases. Tissue barriers 2013;1:e24978.

33 Gunzel D, Yu AS: Claudins and the modulation of tight junction permeability. Physiological reviews 2013;93:525-569.

34 Amasheh S, Milatz S, Krug SM, Bergs M, Amasheh M, Schulzke JD, Fromm M: Na+ absorption defends from paracellular back-leakage by claudin-8 upregulation. Biochemical and biophysical research communications 2009;378:45-50.

35 Fujita H, Sugimoto K, Inatomi S, Maeda T, Osanai M, Uchiyama Y, Yamamoto Y, Wada T, Kojima T, Yokozaki H, Yamashita T, Kato S, Sawada N, Chiba H: Tight junction proteins claudin-2 and -12 are critical for vitamin d-dependent ca2+ absorption between enterocytes. Molecular biology of the cell 2008;19:1912-1921.

36 Wada M, Tamura A, Takahashi N, Tsukita S: Loss of claudins 2 and 15 from mice causes defects in paracellular na+ flow and nutrient transport in gut and leads to death from malnutrition. Gastroenterology 2013;144:369-380.

Figure legends

Figure 1 Schematic representation of the CKO strategy for the mouse Npt2b gene.

A: A vector targeting the *Npt2b* gene was constructed by inserting loxP and Frt with a neo cassette on a BAC genomic clone. Correctly targeted ES cell clones were used to establish *Npt2b* conditional knockout (CKO) mouse lines. After recombination by Cre between the two loxP sites, the genomic region including exon 5 to exon 6 was inverted, and the spliced pattern was confirmed by mRNA analysis using primer set sNpt2b listed in Table 2. Spliced donor (SD), Spliced acceptor (SA) **B**: Representative results of genotyping PCR. Primer sets to detect the CKO alleles and the CAG-*MerCreMer* transgenic allele are listed in Table 1. **C**: Predicted reverse transcription PCR analysis in intestine for detection of null (△) or wild-type (WT) using primer set sNpt2b. NC: negative control. **D**: Western blotting analysis of brush-border membrane vesicles (BBMVs) isolated from the proximal and distal intestine from control and Npt2b CKO mice. Each lane was loaded with 20 μg BBMV. Actin was used as an internal control.

Figure 2 Physiologic data of Npt2b conditional knockout mice

Metabolic cages were used for 24-h urine and feces collection from WT and Npt2b CKO mice at 10 wk of age (n=6-14), values are mean ± SE. **P*<0.05 vs. control mice.

Figure 3 Intestinal and renal brush-border membrane Pi transport activity in Npt2b conditional knockout mice

Na^+-independent and Na^+-dependent Pi transport activity in the proximal (**A**) and distal (**B**) intestine BBMVs of mice (n=3-6). **C**: Na^+-dependent Pi transport activity in the renal BBMVs of mice (n=3-6). Values are means ± SE. **P*<0.05 vs. control mice. **D**: Western blot analysis of the renal type II Na/Pi cotransporter

protein, Npt2a and Npt2c. Data were normalized to actin expression. Male 10-wk-old mice (n=4) were used. Values are mean ± SE.

Figure 4 Intestinal luminal Pi concentration in wild-type mice

Luminal Pi concentration levels in proximal, middle, and distal intestine of wild-type mice.

A: Pi concentration at 11:00 in the morning and 11:00 at night following Marks's protocol[17] and **B:** Pi concentration at the same time-points collected using the cotton ball wiping protocol, which is a modification of Masaoka's[18] and Tanaka's[19] protocol. Data are represented as means ± SE. **P*<0.05, ***P*<0.01, n=4-6.

Figure 5 Intestinal Pi transport activity based on everted sac study

Uptake of ^{32}P to the vascular side was measured in mouse everted intestine. Each sac was incubated with 0.25 □Ci/ml ^{32}P for 30 min at 37°C (n=3). Data are represented as means ± SE. **P*<0.05, n=4-6. The study was conducted under two conditions. Transport solution contained either 1 mM (A, B) or 4 mM Pi (C, D).

Figure 6 Intestinal transporter mRNA expression and intestinal tight junction structure molecule mRNA expression in Npt2b conditional knockout mice

Real-time PCR for intestinal transporter and claudin mRNA expression (n=3-5). Relative intensity data are represented as mean ± SE. ^{a}P<0.05 vs proximal intestine of the same group, **P*<0.05, $^{\#}P$<0.01 vs control group.

Figure 7 Tight junction structure protein expression in Npt2b conditional knockout mice

Western blotting for claudin protein expression in distal intestine of mice. Data are mean ± SE. $^{*}P$<0.05.

A

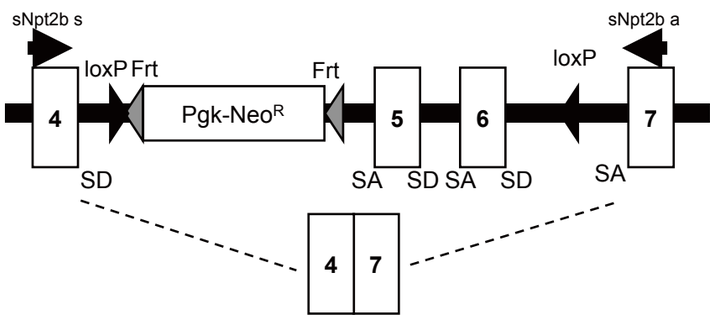
sNpt2b s
loxP Frt
Pgk-Neo^R
Frt
loxP
sNpt2b a
4
5
6
7
SD
SA SD SA SD
SA
4 7

B

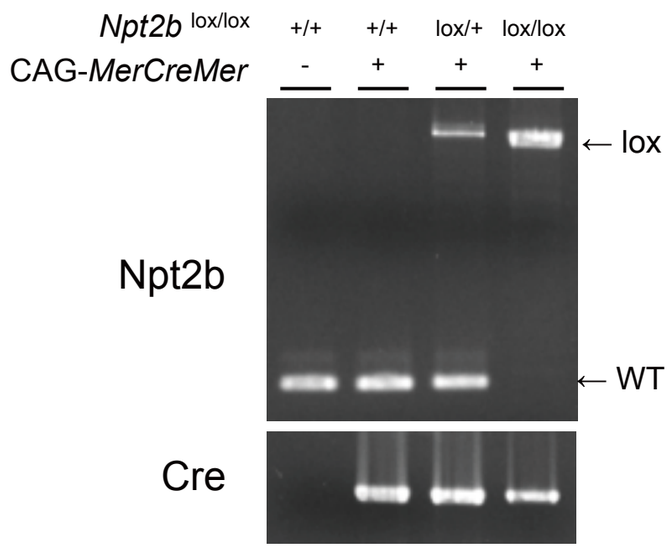
Npt2b lox/lox
+/+ +/+ lox/+ lox/lox
CAG-*MerCreMer*
- + + +
Npt2b
← lox
← WT
Cre

C

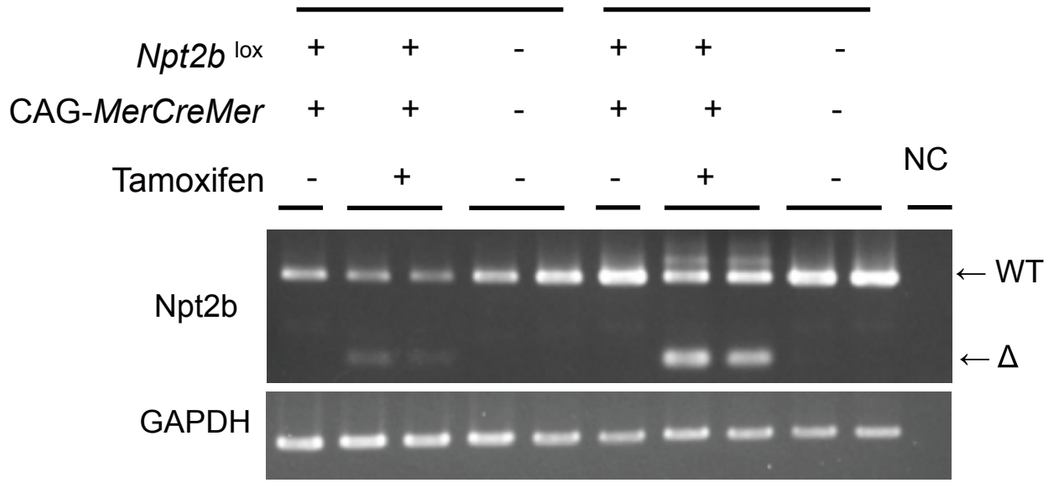
Proximal intestine
Distal intestine
Npt2b lox + + - + + -
CAG-*MerCreMer* + + - + + -
Tamoxifen - + - - + -
NC
Npt2b
← WT
← Δ
GAPDH

D

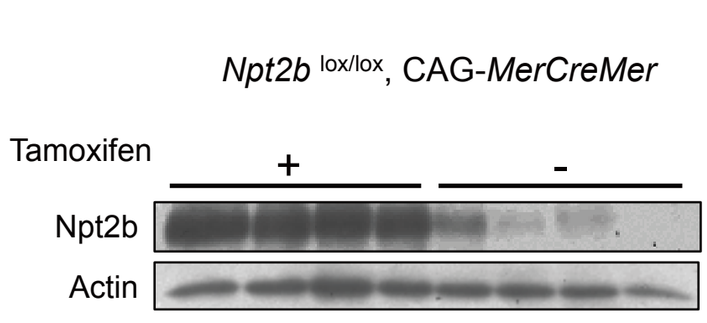
Npt2b lox/lox, CAG-*MerCreMer*
Tamoxifen
+
-
Npt2b
Actin

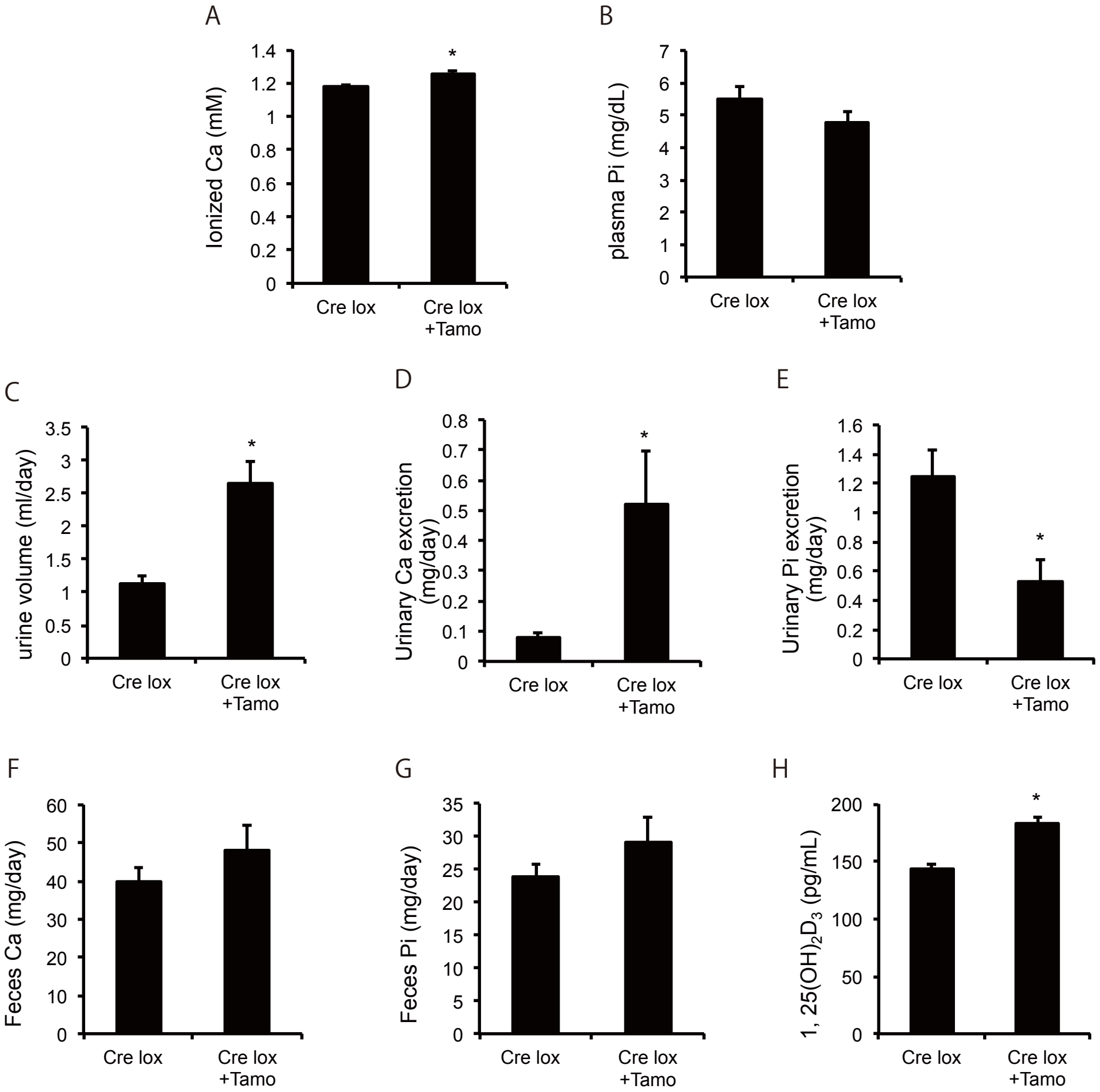
A
Ionized Ca (mM)
1.4
1.2
1
0.8
0.6
0.4
0.2
0
*
Cre lox
Cre lox +Tamo
B
plasma Pi (mg/dL)
7
6
5
4
3
2
1
0
Cre lox
Cre lox +Tamo
C
urine volume (ml/day)
3.5
3
2.5
2
1.5
1
0.5
0
*
Cre lox
Cre lox +Tamo
D
Urinary Ca excretion (mg/day)
0.8
0.7
0.6
0.5
0.4
0.3
0.2
0.1
0
*
Cre lox
Cre lox +Tamo
E
Urinary Pi excretion (mg/day)
1.6
1.4
1.2
1
0.8
0.6
0.4
0.2
0
*
Cre lox
Cre lox +Tamo
F
Feces Ca (mg/day)
60
50
40
30
20
10
0
Cre lox
Cre lox +Tamo
G
Feces Pi (mg/day)
35
30
25
20
15
10
5
0
Cre lox
Cre lox +Tamo
H
1, 25(OH)2D3 (pg/mL)
200
150
100
50
0
*
Cre lox
Cre lox +Tamo

Figure 2

Figure 3R1

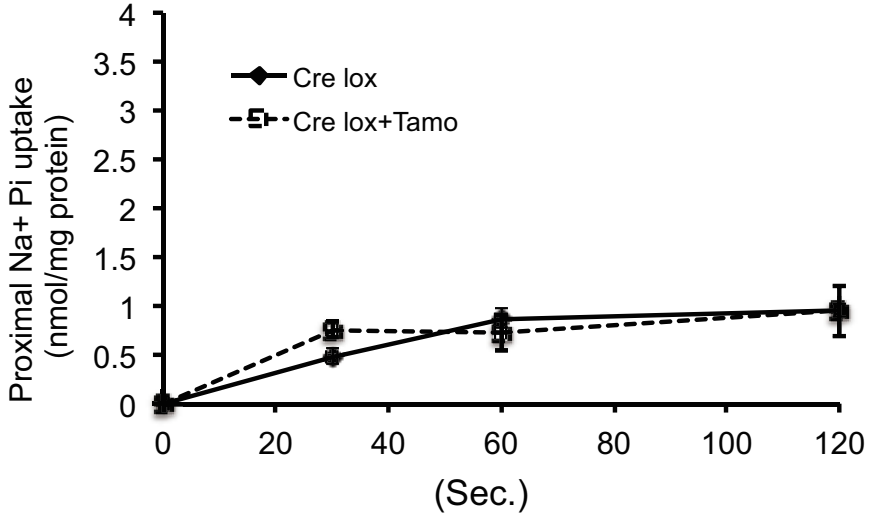
Proximal Na+ Pi uptake (nmol/mg protein)
Cre lox
Cre lox+Tamo
(Sec.)

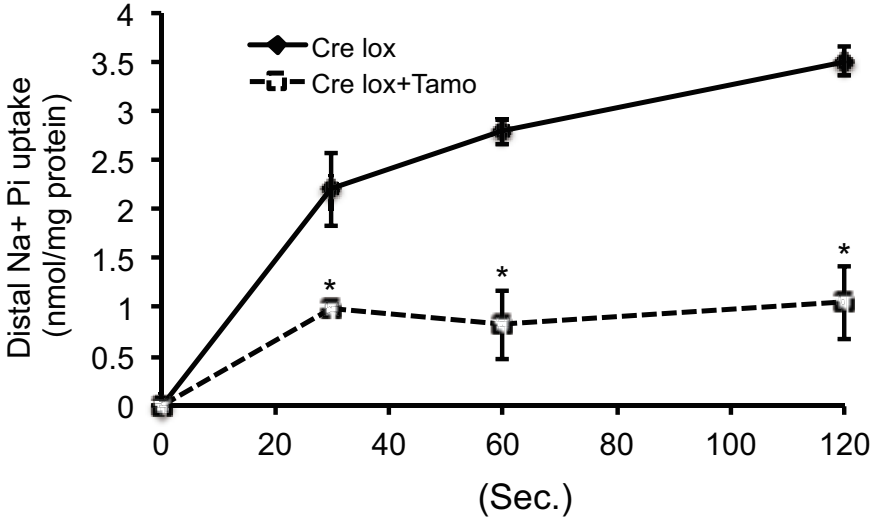
Distal Na+ Pi uptake (nmol/mg protein)
Cre lox
Cre lox+Tamo
(Sec.)

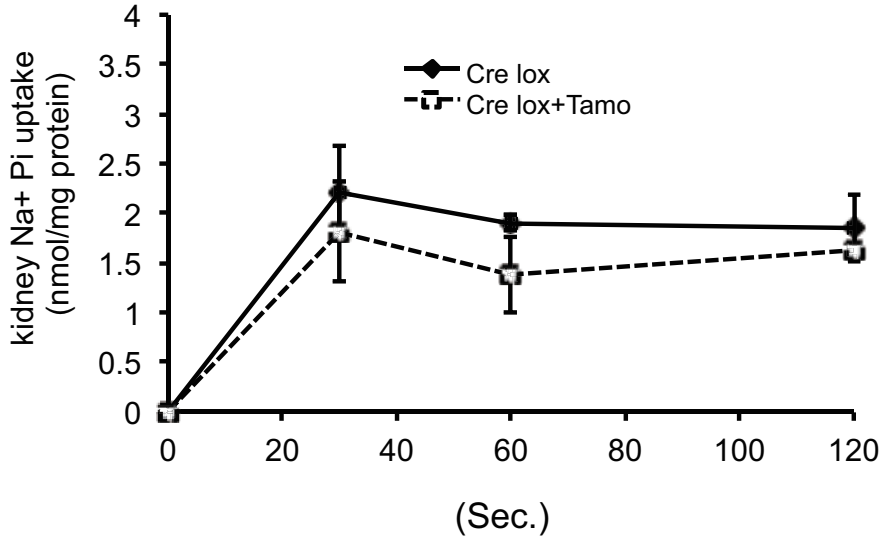
kidney Na+ Pi uptake (nmol/mg protein)
Cre lox
Cre lox+Tamo
(Sec.)

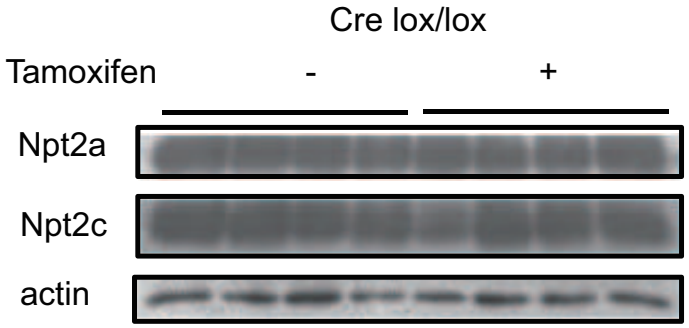
Cre lox/lox
Tamoxifen
-
+
Npt2a
Npt2c
actin

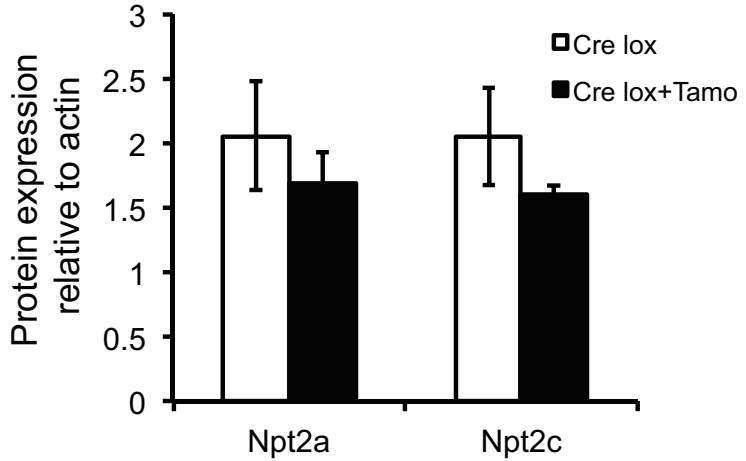
Protein expression relative to actin
Cre lox
Cre lox+Tamo
Npt2a
Npt2c

Figure 4

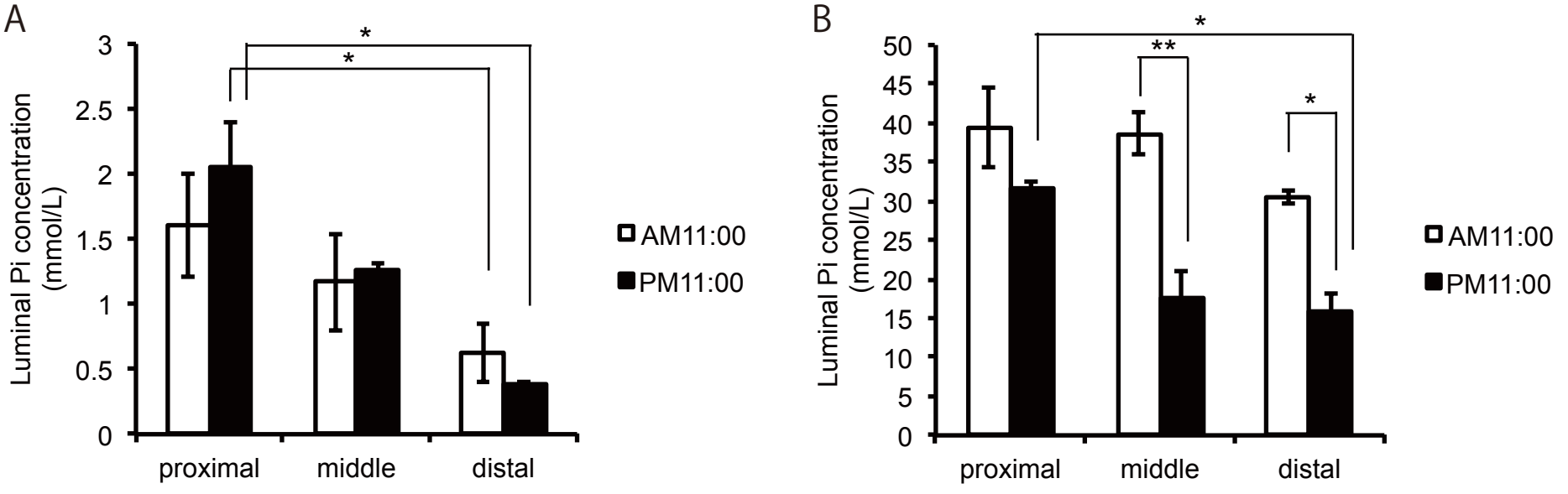

Figure 4

Figure 5

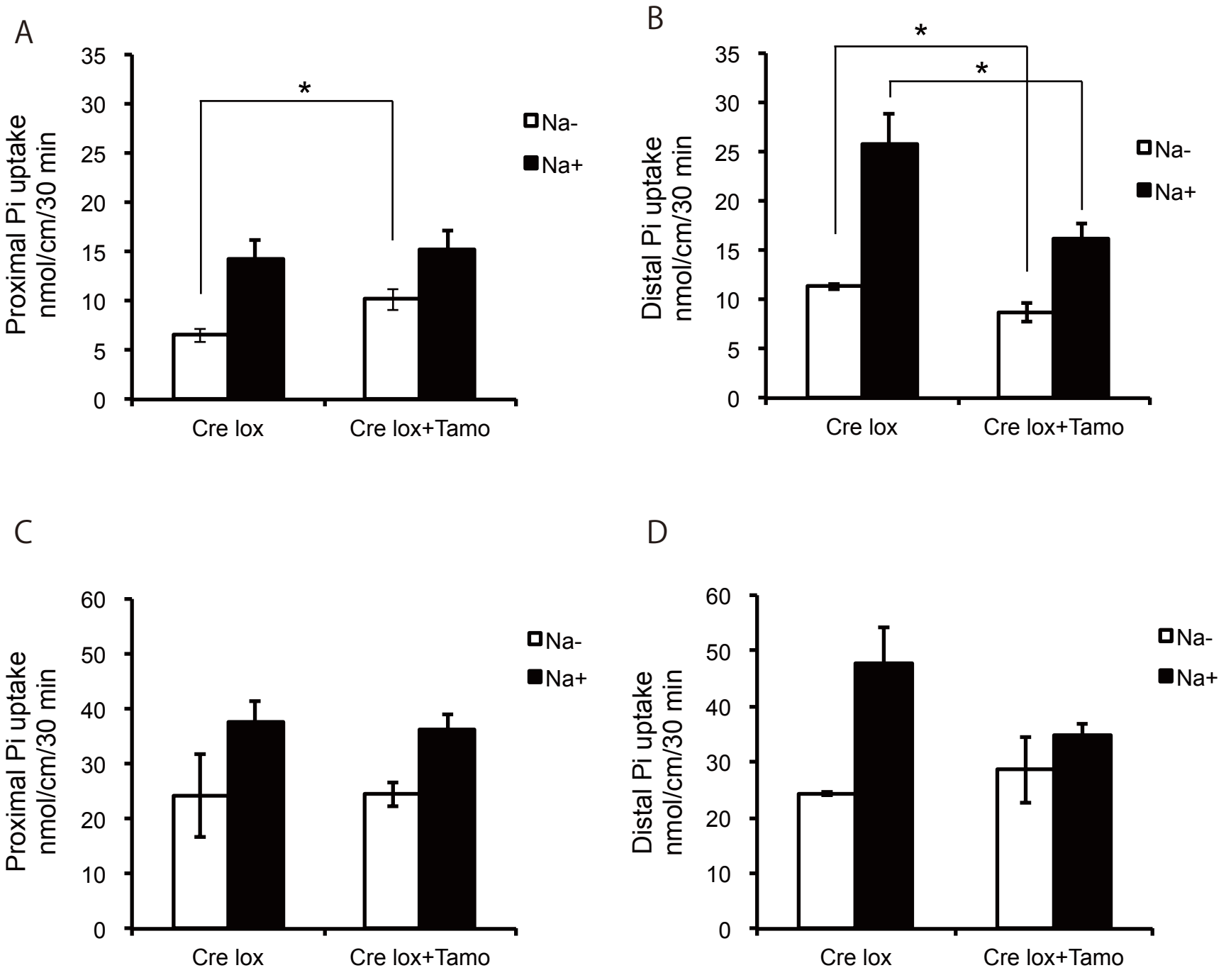

Figure 5

Figure 6

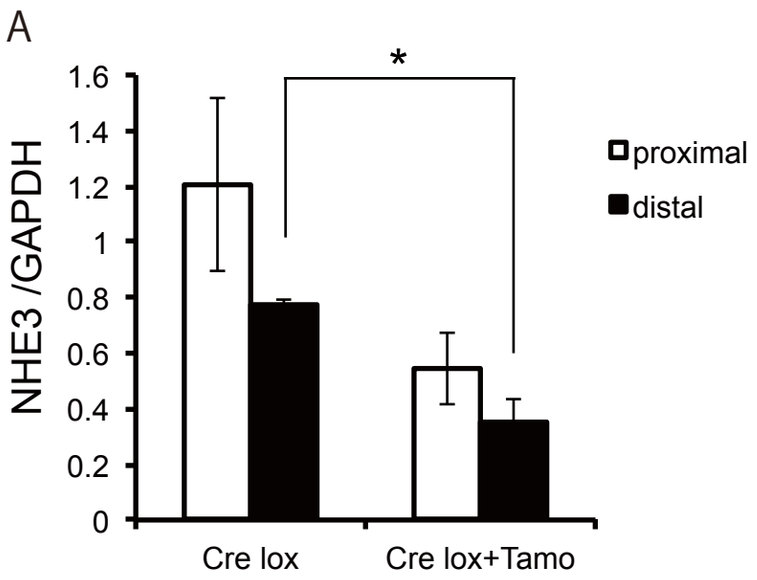

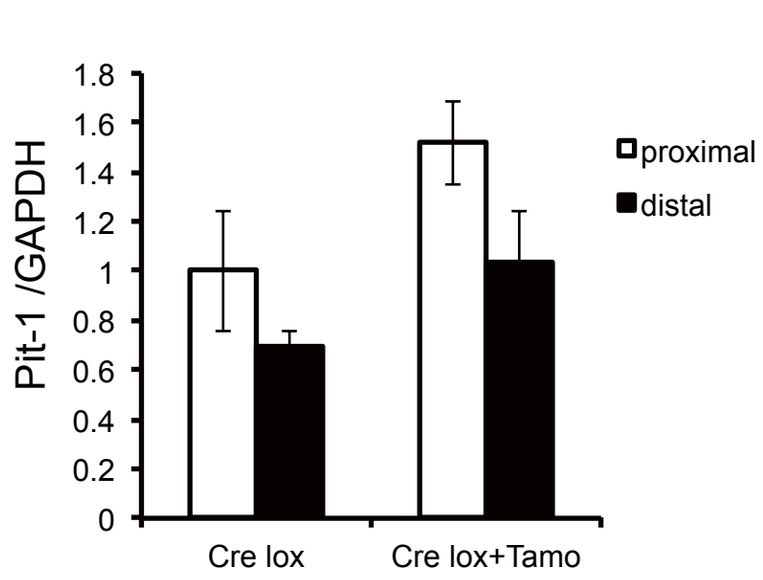

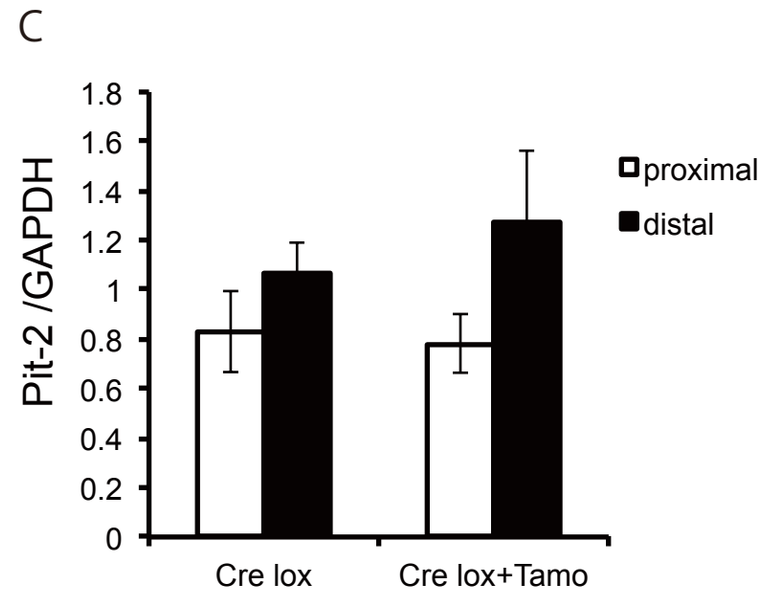

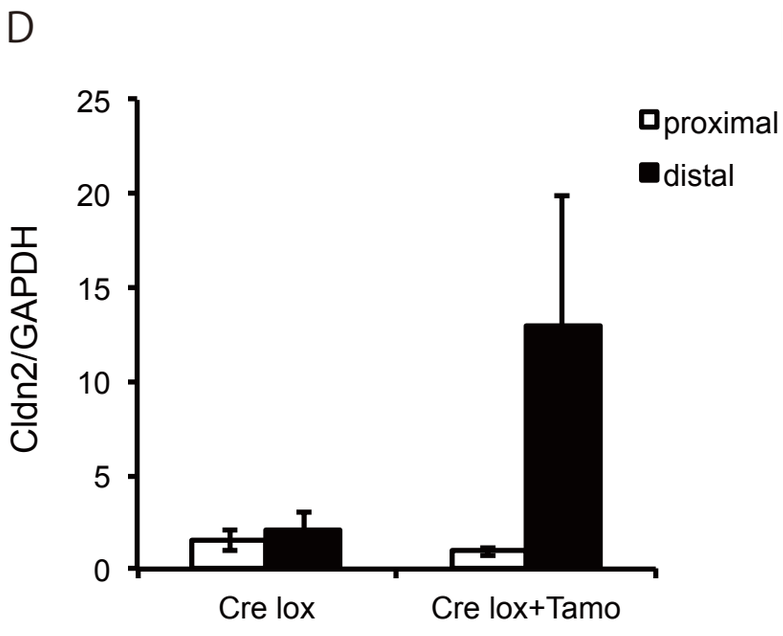

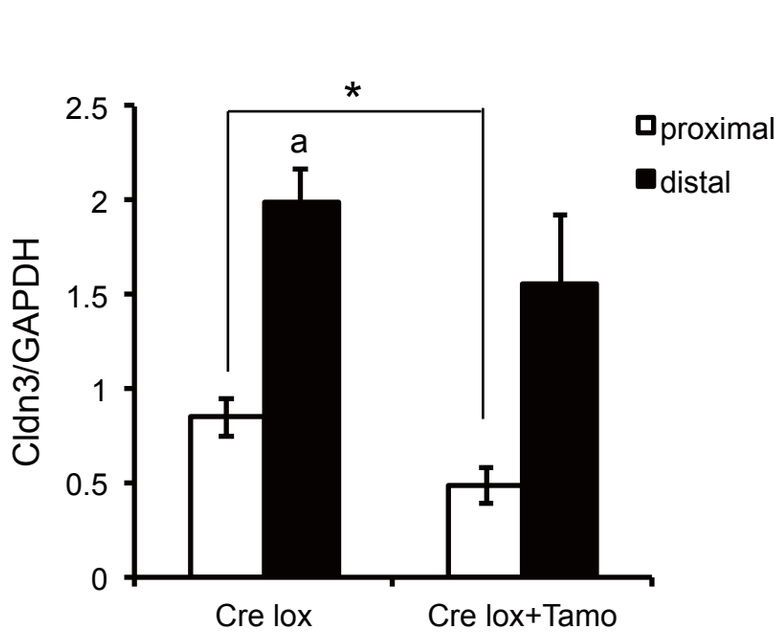

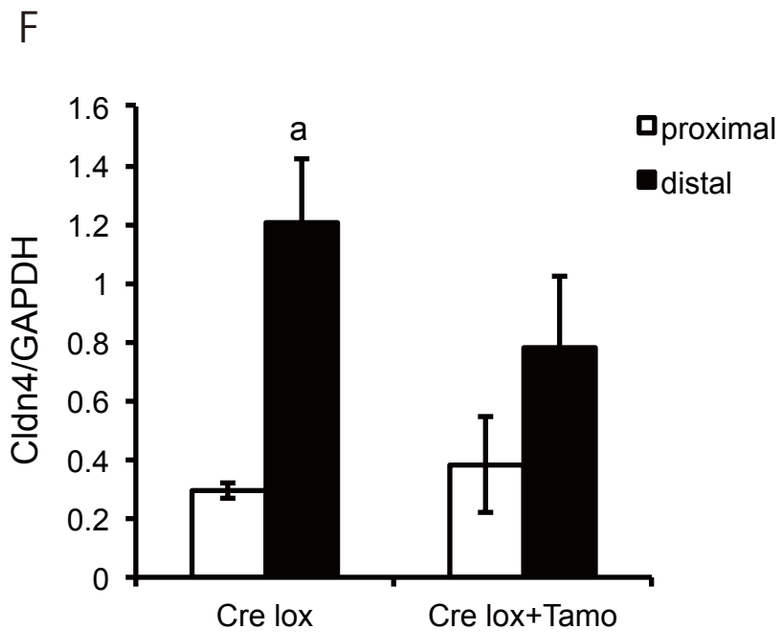

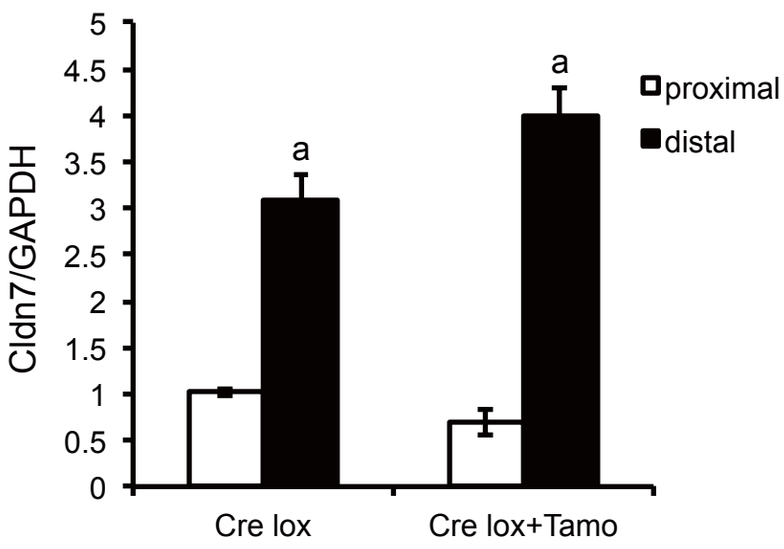

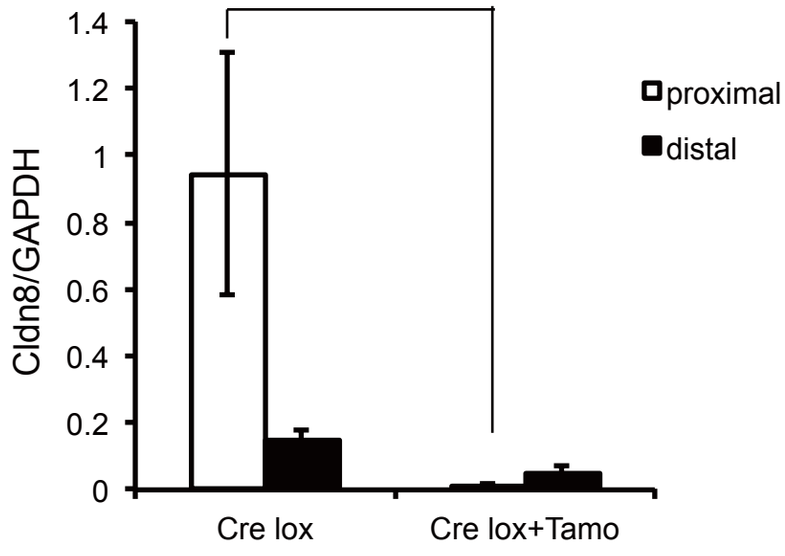

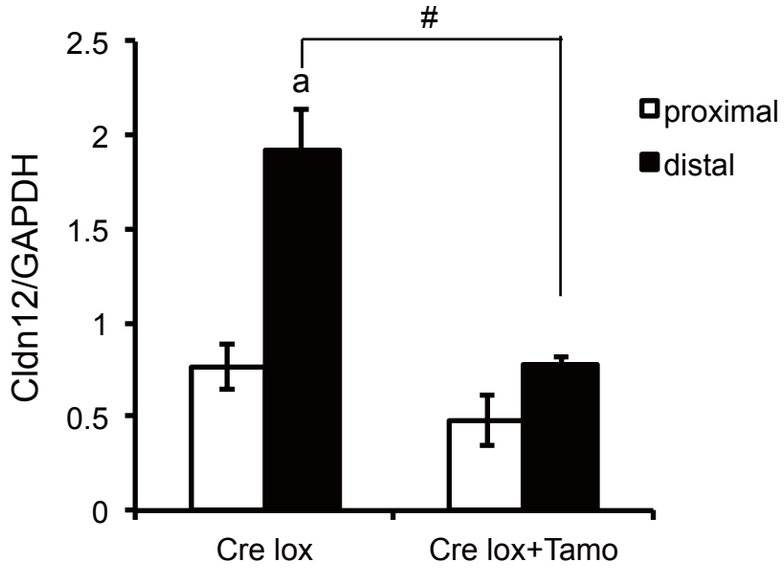

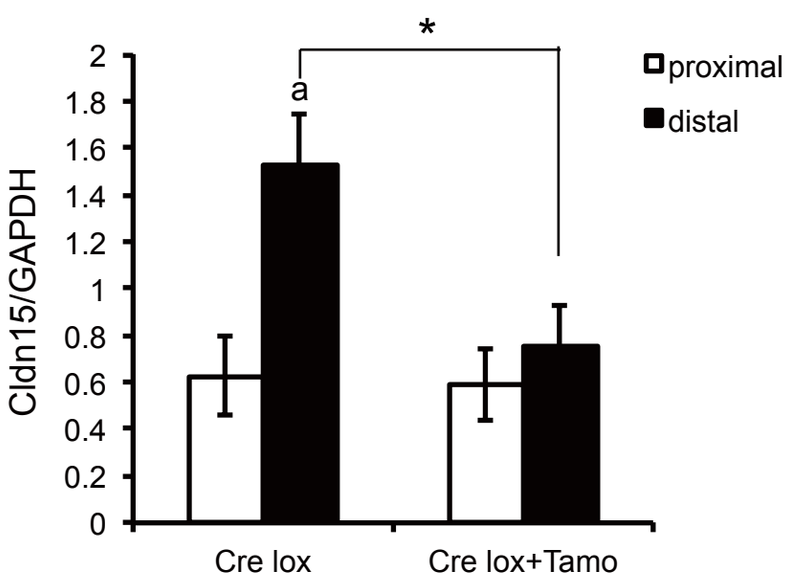

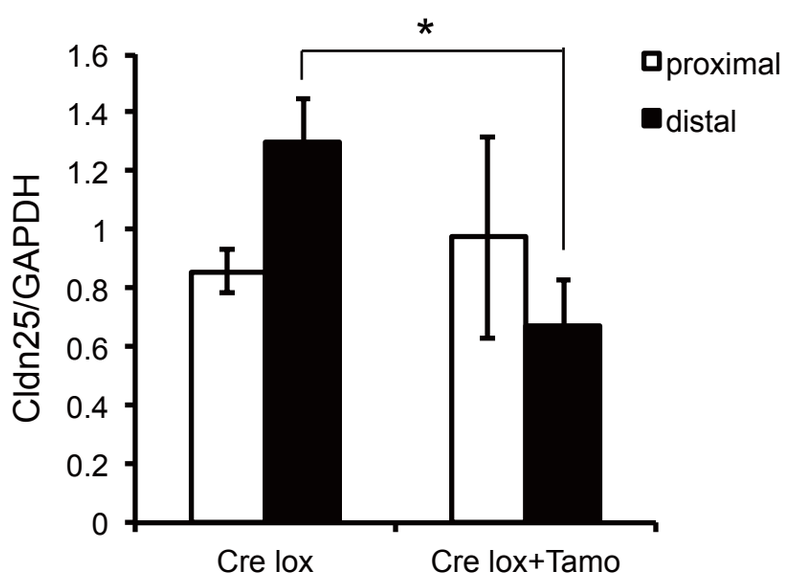

Figure 6

Figure 7

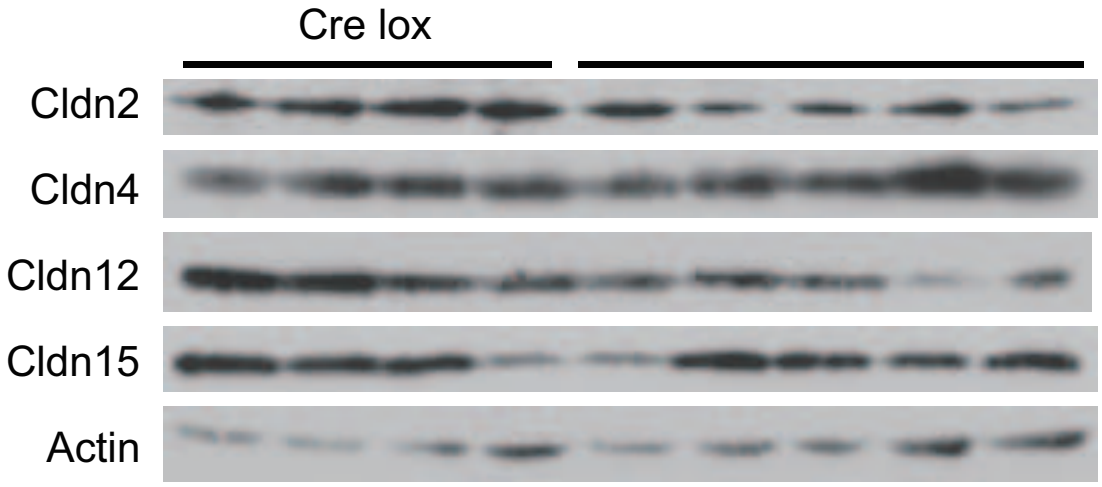

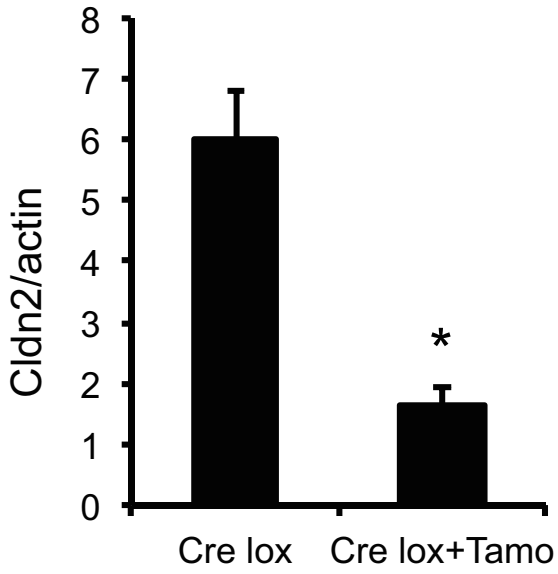

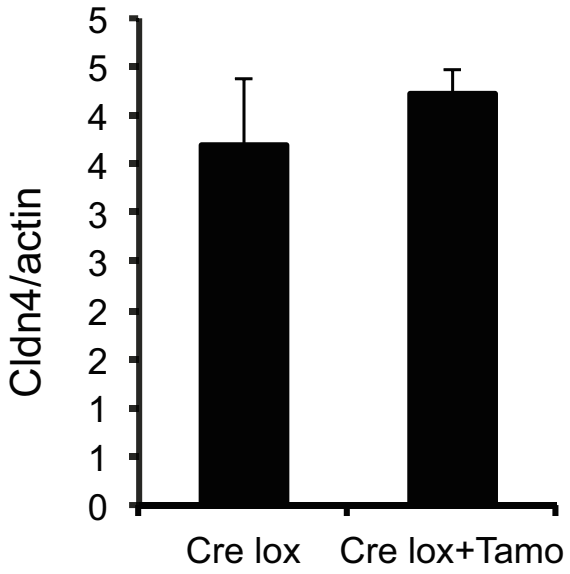

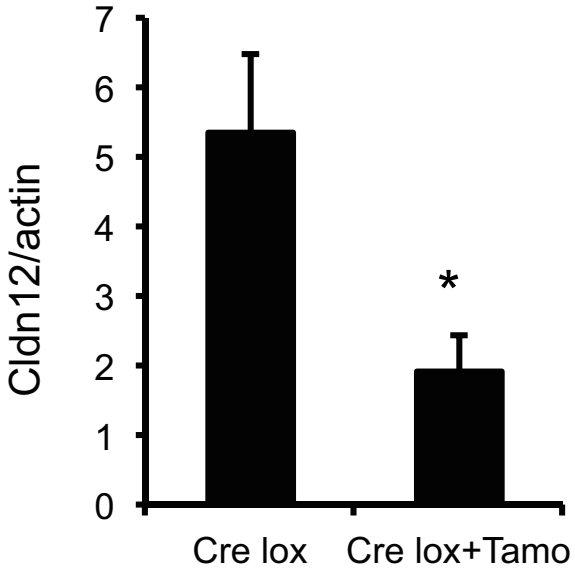

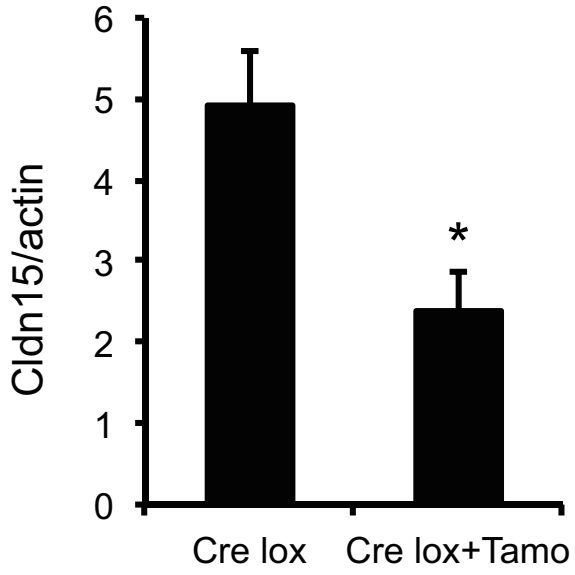

Figure 7

Table

Table 1 Primers for genotyping

name	sense	antisense
MerCreMer Tg allele	AGGCGTTTTCTGAGCATACCTGGA	TCTTCCAGCAGGCGCACCATTG
Conditional KO allele	TGTTGGGGAATAGAGGATCAACT	TGTAGAGTAGGAACCTAGCCCTCA

Table 2 Primers for RT-PCR

name	sense	antisense
sNpt2b	ATGTACTGAGCAGCGCCTTC	CACAAGGTTGGTCAGGATCTC
Npt2b	AGCGCTGATCATGGCTCCTT	CCTGCATAAGCGCCACGATC
Pit-1	CCCATGGACCTGAAGGAGGA	CCATGGGCAAATGACCCAAA
Pit-2	CTCAGAAGGCACGTCAGCAG	TCAGAGGCCAGCCTCATTTC
NHE3	GCATAGTGTCCTTCTTCGTG	GGCTCGATGATACGCACATG
claudin-2	GCAAACAGGCTCCGAAGATACT	GAGATGATGCCCAAGTACAGAG
claudin-3	CACCACTACCAGCAGTCGATGAAC	AGACTGTGTGTCGTCTGTCACCATC
claudin-4	GGTAGCTCAGCTGTGACTTTGGACTC	CTGGAGTAACGTGTAGGCTGAGTGAG
claudin-7	ACGCCCATGAACGTTAAGTACGAG	CTTTGCTTTCACTGCCTGGACA
claudin-8	CTGGGGATAAAAGAGAAGGAGGCTGA	AGGCTGCAAAGCAGGATAGCAGAAAG
claudin-12	CAGACCAGTGTGTACTCAGACTTTCTACCC	GAAGCAACATACTGACTGTCTCCTGACG
claudin-15	CATCTTTGAGAACCTGTGGTACAGC	GATGGCGGTGATCATGAGAGC
claudin-25	ACGAGCAGTTCATGGAGAAG	CAAAGCACATCAAGCCCAAG
GAPDH	CTGCACCACCAACTGCTTAGC	GCCTGCTTCACCACCTTCTTG